Tensile Biomechanical Properties of Human Temporomandibular Joint Disc: Effects of Direction, Region and Sex

Gregory J. Wright[1], **Matthew C. Coombs**[1,2], **R. Glenn Hepfer**[1], **Brooke J. Damon**[1,2], **Thierry H. Bacro**[3], **Michael K. Lecholop**[4], **Elizabeth H. Slate**[5], and **Hai Yao**[1,2]

[1]Department of Bioengineering, Clemson University, Clemson, SC

[2]Department of Oral Health Sciences, Medical University of South Carolina (MUSC), Charleston, SC

[3]Center for Anatomical Studies and Education, MUSC, Charleston, SC

[4]Department of Oral & Maxillofacial Surgery, MUSC, Charleston, SC

[5]Department of Statistics, Florida State University, Tallahassee, FL

Abstract

Approximately 30% of temporomandibular joint (TMJ) disorders include degenerative changes to the articular disc, with sex-specific differences in prevalence and severity. Limited tensile biomechanical properties of human TMJ discs have been reported. Stress relaxation tests were conducted on TMJ disc specimens harvested bilaterally from six males and six females (68.9 ± 7.9 years), with step-strain increments of 5%, 10%, 15%, 20% and 30%, at 1% strain-per-second. Stress versus strain plots were constructed, and Young's Modulus, Instantaneous Modulus and Relaxed Modulus were determined. The effects of direction, region, and sex were examined. Regional effects were significant ($p<0.01$) for Young's Modulus and Instantaneous Modulus. Anteroposteriorly, the central region was significantly stiffer than medial and lateral regions. Mediolaterally, the posterior region was significantly stiffer than central and anterior regions. In the central region, anteroposteriorly directed specimens were significantly stiffer compared to mediolateral specimens ($p<0.04$). TMJ disc stiffness, indicated by Young's Modulus and Instantaneous Modulus, were higher in directions corresponding to high fiber alignment. Additionally, human TMJ discs were stiffer for females compared to males, with higher Young's Modulus and Instantaneous Modulus, and female TMJ discs relaxed less. However, sex effects were not statistically significant. Using second-harmonic generation microscopy, regional collagen fiber organization was identified as a potentially significant factor in determining the biomechanical properties for any combination of direction and region. These findings establish

Address for Correspondence: Hai Yao, PhD, Department of Bioengineering, Clemson University, CU-MUSC Bioengineering Program, 173 Ashley Avenue, MSC 508, Charleston, SC 29425, Phone: (843)876-2380, Fax: (843)792-6626, haiyao@clemson.edu.

CONFLICT OF INTEREST

None of the authors of this paper have a conflict of interest that might be construed as affecting the conduct or reporting of the work presented.

structure-function relationships between collagen fiber direction and organization with biomechanical response to tensile loading, and may provide insights into the prevalence of TMJ disorders among women.

Keywords

Temporomandibular joint (TMJ); TMJ disc; Tensile biomechanics; Viscoelasticity

INTRODUCTION

Over half the population over age 50 shows radiographic evidence of degenerative changes to their temporomandibular joints (TMJs), increasing to 85% by age 75 (Haskin et al., 1995; Lawrence, 1987; Moskowitz, 1988; Peyron and Altman, 1992). Individuals seeking treatment for temporomandibular symptoms is approximately 2-4% of the total population (Haskin et al., 1995), with approximately 30% of all temporomandibular joint disorders (TMJDs) including degenerative changes to the articular disc (Ahmad et al., 2009; Schiffman et al., 2010). Sex-specific differences exist in TMJDs, with women predominately affected with greater severity of symptoms (LeResche, 1997; Warren and Fried, 2001). Biomechanical factors such as joint architecture and tissue mechanical quality may be predictive of TMJD development and progression, similar to other joints showing sex-based differences among young patient populations (Ford et al., 2010a; Ford et al., 2010b; Griffin et al., 2000; Hughes et al., 2008; Kernozek et al., 2005).

The TMJ disc is located between the head of the mandibular condyle and articular eminence of the glenoid fossa. During jaw opening and closing, the disc translates anteroposteriorly with the condyle (Piette, 1993), supported by anterior attachments to the lateral pterygoid muscle, anterior insertions into the condyle, and posterior attachments to the retrodiscal tissue (Tanaka and van Eijden, 2003). As a result of translation, the disc experiences tension as it is stretched anteroposteriorly and mediolaterally over the condyle (Gallo et al., 2000; Osborn, 1985; Rayne, 1987).

Described as biconcave (Taguchi et al., 1980), the disc is divided into an anterior band, intermediate zone, and posterior band (Rees, 1954). The disc is thicker medially than laterally, while anteroposteriorly the disc is thinnest in the intermediate zone and thickest in the posterior band (Choukas and Sicher, 1960; Griffin et al., 1975; Hansson et al., 1977; Shapiro, 1950; Wang et al., 2009). The disc is comprised of strong, interwoven collagen bundles, predominately in the anteroposterior direction, interlaced with mediolaterally oriented fibers in the anterior and posterior bands (Scapino, 1983). Fibers are tightly bound in the intermediate zone, and loosely bound with irregular orientation in the anterior and posterior bands (Jagger, 1980).

Limited tensile biomechanical properties of the TMJ disc have been reported. Detamore and Athanasiou (2003) reported increased elastic moduli, toughness and strength in varying directions and regions of porcine disc, corresponding to differences in collagen fiber orientation. Young's Modulus also shows direction and region dependent affects (Matuska et al., 2016; Shengyi and Xu, 1991; Tanne et al., 1991). However, the available literature

provides an incomplete tensile profile of the TMJ disc, relying heavily upon animal tissue and reporting a wide range of properties. While animal models are accepted, and human and porcine TMJ discs are considered similar in size, shape and masticatory pattern (Herring et al., 2002; Kalpakci et al., 2011; Mills et al., 1994), care must be taken in applying animal data as a benchmark for tissue engineered constructs or biomechanical modeling. Additionally, human discs allow for sex dependencies in tissue mechanical quality to be investigated, potentially identifying etiological factors for the increased prevalence of TMJDs among women.

Given region and direction dependencies reported for porcine TMJ discs, correlated to regional collagen fiber orientation and organization, the objectives of this study were to determine (1) direction, (2) region and (3) sex dependent biomechanical properties of human TMJ discs. Tensile biomechanical tests were performed on human TMJ discs following the test protocol laid out by Detamore and Athanasiou (2003) for porcine TMJ discs. By following the same test protocol, it was possible to directly compare biomechanical outcomes and evaluate the biomechanical similarity between human and porcine TMJ discs. Regional variations in disc response were investigated with pairwise comparisons within each direction, and comparison of centrally located specimens in the anteroposterior and mediolateral directions. Regional collagen fiber orientation and organization were evaluated using second-harmonic generation microscopy, a significant advancement over traditional histological or imaging techniques, capable of imaging intact and unstained tissues (Chen et al., 2012; Houle et al., 2015; Lilledahl et al., 2015). Sex dependent biomechanical differences were anticipated, supported by sex specific differences in human temporomandibular disc electrical conductivity, porosity and ion diffusivity (Wright et al., 2013), potentially explaining the differences in the prevalence and severity of TMJDs among women.

METHODS

Specimen selection and preparation

Human TMJ discs were harvested in the MUSC Gross Anatomy Laboratory under institutional approval. Donor tissues were fresh frozen, and never formalin fixed. After removal, TMJ discs were photographed, morphologically screened to select healthy bilateral discs, wrapped in cellophane and gauze soaked with PBS with protease inhibitors, placed in specimen bags and frozen until use at −20 °C. Discs exhibiting physical signs of trauma, including fissures or bruises, were excluded. In total, twenty-four morphologically normal TMJ discs were harvested bilaterally from twelve donors, six males (67.5 ± 8.4 years) and six females (70.3 ± 8.7 years).

Left articular discs were used for anteroposterior tensile tests, and right articular discs were used for mediolateral tests. Specimens were prepared by dissecting three strips from each disc using parallel razor blades with a 2 mm spacer (Figure 1, Left). Anteroposteriorly, specimens were taken at lateral (AP-LAT), central (AP-CENT), and medial (AP-MED) regions. Mediolaterally, specimens were taken at anterior (ML-ANT), central (ML-CENT), and posterior (ML-POST) regions. Specimens were removed with equal spacing, avoiding peripheral attachments. Immediately after dissection, tissue strips were transferred to a

microtome, removing the inferior and superior portions of each sample to eliminate biconcavity and ensuring even parallel cross-sections (Figure 1, Right). Specimens were measured for thickness using a current sensing micrometer prior to testing. Specimens had an average thickness of 2.2 ± 0.5 mm in the anteroposterior direction and 2.5 ± 0.6 mm in the mediolateral direction.

Tensile testing

Incremental stress relaxation tests were conducted using a materials test system (ElectroForce 3200, Bose, Eden Prairie, MN). A custom enclosed chamber maintained a constant test environment of 0.15 M PBS at 37 °C during testing (Figure 2, Left). The PBS bath was replaced after each test. Specimens were gripped by custom tensile clamps using fine grit sandpaper (Figure 2, Right). A 0.05 N tare load was applied to each specimen, corresponding to approximately 9 kPa (Detamore and Athanasiou, 2003; Elliott and Setton, 2001), and an initial length was determined as the grip-to-grip distance at tare load. Initial specimen lengths were 7.1 ± 1.8 mm and 10.6 ± 4.1 mm in the anteroposterior and mediolateral directions, respectively. Specimen strain during testing was determined by the change in grip-to-grip distance divided by initial specimen length. Specimen stress was calculated as the force recorded by the materials test system divided by specimen cross-sectional area determined from initial width and thickness measurements. Tensile clamp buoyancy forces were subtracted out.

Specimens were preconditioned before each stress-relaxation test with 10 cycles between 0-2% strain, with a strain rate of 0.2% strain-per-second. Preliminary tests showed disc specimens reached steady-state forces within nine cycles. Following preconditioning, specimens were loaded in step-strain increments of 5%, 10%, 15%, 20% and 30% strain, with relaxation periods of 15, 15, 15, 20, and 30 minutes (Figure 3, Left). Ramp strains were applied at 1% strain-per-second. Relaxation times were based on preliminary tests to ensure stress equilibrium was reached. Specimens with a detected slip during testing were retested. The study followed the methods established by Detamore and Athanasiou (2003) for incremental stress-relaxation tensile tests of porcine TMJ disc tissues.

Biomechanical analysis

Stress-versus-strain plots were constructed for each incremental stress relaxation test (Figure 3, Right). Young's Modulus was calculated as the slope of the best-fit line through 40-100% of the stress-strain curve during the ramp-loading phase for each strain increment. Instantaneous and Relaxed Moduli were calculated as the slope of the best fit lines through the local maxima and minima (Detamore and Athanasiou, 2003), corresponding to the local peaks of the stress-strain curves and the end of each stress relaxation phase, respectively. Biomechanical analysis was performed using MATLAB (MATLAB R2016a, The MathWorks Inc., Natick, MA).

Tissue micro-structure analysis

To determine tissue microstructure, the superior surface of an intact human TMJ disc was imaged using second-harmonic generation microscopy (Chen et al., 2012; Houle et al., 2015; Lilledahl et al., 2015). The disc was dissected from a fresh-frozen 73-year-old female

cadaver, frozen until use at −20 °C. Prior to imaging, the intact disc was thawed and mounted on a 35 mm glass bottom dish (MatTek, Ashland, MA). The disc was never stained or sectioned prior to imaging. Imaging was performed using an Olympus Fluoview 1200 MPA (Olympus, Center Valley, PA), with a 30x oil immersion objective lens (UPLSAPO, 30XSIR; Olympus, Center Valley, PA). The excitation laser was at a wavelength of 860 nm, and the signal was collected in the 420-460 nm range. Image resolution was 1024×1024 with a field of view of 423×423 μm.

Statistical analysis

Statistical modeling focused on assessing differences in Instantaneous Modulus and Relaxed Modulus among disc region (AP-LAT, AP-CENT, AP-MED, ML-ANT, ML-CENT, ML-POST), and differences in Young's Modulus among disc region and strain increment (5%, 10%, 15%, 20% and 30%). Linear mixed effects models for each outcome incorporated these predictors, as well as donor sex and age, together with random effects for donor and direction (anteroposterior or mediolateral) to accommodate within-donor and within-direction correlation. Model comparison via likelihood ratio testing supported within-donor correlation for Instantaneous Modulus and Relaxed Modulus. Young's Modulus additionally exhibited significant within-region correlation. Heterogeneity of the variance of Young's Modulus was modeled as region-specific residual variation. In all cases, neither donor sex nor donor age contributed significantly, hence these predictors were dropped from the final models. Seven contrasts among disc region were evaluated: pairwise within the anteroposterior (AP-MED vs AP-CENT vs AP-LAT) and mediolateral (ML-ANT vs ML-CENT vs ML-POST) directions, and between the central regions in the anteroposterior and mediolateral directions (AP-CENT vs ML-CENT), and all pairwise differences among the five strain increments for Young's Modulus, with Holm (1979) adjustment for multiple comparisons. Analyses were performed in SAS v. 9.4 with SAS/STAT 13.1.

RESULTS

Young's Modulus

Young's Modulus showed significant differences by region (p<0.001) and strain increment (p<0.001) (Figure 4). The interaction between region and strain increment was not significant. In the anteroposterior direction, Young's Modulus, adjusted for strain increment, was significantly higher in the AP-CENT region compared to both AP-LAT (p=0.04) and AP-MED (p<0.001) regions. In the mediolateral direction, Young's Modulus, adjusted for strain increment, was significantly lower in the ML-CENT region compared to both ML-POST (p<0.001) and ML-ANT (p=0.04) regions, and ML-ANT was significantly less than ML-POST (p=0.04). In the central region of the articular disc, Young's Modulus was significantly higher in the anteroposterior direction compared to the mediolateral direction (p=0.04). Young's Modulus varied significantly by strain increment for all pairwise comparisons (p<0.01), except between 10-30% (p=0.087) and 15-20% (p=0.985) strain which were not significantly different. With increasing strain increment, Young's Modulus increased from 0-15% strain, plateauing between 15-20%, before decreasing at 30% strain (Figure 4). Average Young's Modulus was higher for females (14.3 ± 8.5 MPa) compared to males (11.2 ± 6.8 MPa), however not significantly (p=0.276) (Table 1).

Instantaneous Modulus

Differences in Instantaneous Modulus by region were significant (p=0.007) (Figure 5). Anteroposteriorly, AP-CENT specimens had higher Instantaneous Modulus compared to AP-MED specimens, however not significantly (p=0.068). In the mediolateral direction, ML-POST specimens had significantly higher Instantaneous Modulus compared to ML-CENT specimens (p=0.002). In the central region of the articular disc, Instantaneous Modulus was significantly higher in the anteroposterior direction compared to the mediolateral direction (p=0.001). Instantaneous Modulus was higher for females (8.4 ± 4.1 MPa) compared to males (7.0 ± 3.1 MPa), however not significantly (p=0.383) (Table 1).

Relaxed Modulus

Differences in Relaxed Modulus by region were not significant (p=0.094) (Figure 5). In the anteroposterior direction, AP-CENT specimens had higher Relaxed Modulus than AP-MED and AP-LAT specimens. In the mediolateral direction, ML-POST specimens had higher Relaxed Modulus compared to ML-CENT specimens. Relaxed Modulus in the central region of the articular disc was higher for AP-CENT specimens compared to ML-CENT specimens. Relaxed Modulus was higher for females (4.1 ± 2.3 MPa) compared to males (3.2 ± 1.5 MPa), however not significantly (p=0.264) (Table 1).

Tissue micro-structure

Second-harmonic generation microscopy revealed regional variations in collagen fiber orientation and organization (Figure 6). In the central region of the disc, collagen fibers run predominately anteroposteriorly, and were tightly bound. In the anterior and posterior bands, collagen fibers were predominately mediolaterally directed, with some anteroposteriorly directed fibers interwoven, forming a ring-like periphery. On the medial and lateral aspects of the disc, fibers were predominately in the anteroposterior direction continuing the ring-like periphery of the anterior and posterior bands, with some mediolaterally oriented fibers.

DISCUSSION

The human TMJ disc showed significant direction and region dependent differences in tensile biomechanical properties, in addition to sex dependent trends. These results confirm the anisotropic behavior of the human TMJ disc, with differences in material properties corresponding to principle fiber orientation and organization in each region. Articular disc stiffness, indicated by Young's Modulus and Instantaneous Modulus, were significantly higher in directions corresponding to high fiber alignment. In the central region, the TMJ disc was stiffest in the AP direction and least stiff in the ML direction, corresponding to principally anteroposteriorly oriented fibers. The anterior and posterior bands in the ML direction were both stiffer than the central region. The wide and thick posterior band was stiffest in the mediolateral direction, and was not different across multiple parameters than specimens in the anteroposterior direction.

Second-harmonic generation microscopy, capable of imaging intact unstained collagen fiber orientation and organization (Chen et al., 2012; Houle et al., 2015; Lilledahl et al., 2015), revealed regional variations in human TMJ disc fiber orientation and organization, similar to

that reported for porcine TMJ discs using polarized light microscopy and scanning electron microscopy (Detamore and Athanasiou, 2003; Shi et al., 2013). In the central region of the disc, collagen fibers run predominately in the anteroposterior direction and were tightly bound, supporting a primary direction of stretching in the anteroposterior direction during joint articulation. In the anterior and posterior bands, collagen fibers were predominately mediolaterally directed, with some anteroposteriorly directed fibers interwoven, forming a ring-like periphery around the disc. The peripheral ring-like structure of the TMJ disc stiffens the disc by allowing hoop stresses to form, preventing disc prolapse during joint articulation (Piette, 1993). On the medial and lateral aspects of the disc, fibers run predominately in the anteroposterior direction, continuing the ring-like periphery of the anterior and posterior bands, with some mediolaterally oriented fibers. On the medial aspect of the disc, collagen fibers were much less tightly woven than in the central or lateral aspects of the TMJ disc. Diminished fiber organization relative to the lateral aspect likely contributed to the reduced biomechanical response on the medial aspect, suggesting a functional role differentiable between medial and lateral aspects.

In addition to direction and region differences in biomechanical response, female TMJ discs had higher Young's Modulus, Instantaneous Modulus, and Relaxed Modulus compared to males (Table 1). Sex dependent differences however were not significant for Young's Modulus ($p=0.276$), Instantaneous Modulus ($p=0.383$), or Relaxed Modulus ($p=0.264$). Contrasting female and male TMJ articular discs, differences between female and male discs were on the same order of magnitude as differences among regional contrasts. It is currently unknown whether differences in TMJ articular disc mechanical quality is a causative factor in the development and progression of TMJDs, or the physiologically required disc properties to maintain healthy normal TMJ function. Small sex dependent difference in biomechanical response, in addition to sex-dependent differences in transport properties reported for human TMJ discs (Wright et al., 2013), may be attributed to sex-dependent differences in TMJ disc biochemical composition.

In the available tensile biomechanical data for TMJ discs (Table 2), little agreement exists between reported studies, despite similar test protocols. Compared to the available literature, human TMJ discs have a lower Young's Modulus compared to bovine tissue and porcine tissue from older breeder sows (Matuska et al., 2016; Tanaka et al., 2001). Young's Modulus for human TMJ discs was most similar to bovine TMJ discs, compared to older breeder sows, suggesting the proposed porcine ageing model for TMJDs may not be appropriate (Matuska et al., 2016). Instantaneous and Relaxed Moduli were similar to that reported for typical porcine TMJ discs (Detamore and Athanasiou, 2003), however Instantaneous and Relaxed Moduli were an order of magnitude lower from the present study compared to the only other study using human TMJ disc specimens (Tanaka et al., 2000). Given similarities in strain rate and test protocol, differences in reported moduli for human specimens may be the result of specimen dehydration, which was uncontrolled by Tanaka et al. (2000). Similar to Detamore and Athanasiou (2003), tensile biomechanical testing in the present study was performed in a temperature controlled saline bath to maintain disc hydration over the long test protocol.

In addition to similarities between porcine and human TMJ disc size and shape, joint anatomy, masticatory patterns and omnivorous diet (Herring et al., 2002; Kalpakci et al., 2011; Mills et al., 1994), this study indicates similarity in biomechanical response to loading and tissue microstructure between human and porcine TMJ discs. Instantaneous and Relaxed Moduli, compared directly to Detamore and Athanasiou (2003), are of similar magnitudes and directional and regional trends were also similar. In the anteroposterior direction, specimens from the central region were stiffest, however medially located specimens were stiffer than lateral specimens in the porcine disc unlike in humans which show diminished stiffness on the medial aspect. In the mediolateral direction, the central region was the least stiff and the posterior region the stiffest, similar to humans.

Limitations with the present study include the use of a small sample of human TMJ discs from an older population. It should also be considered that specimens were taken from temporomandibular joints from an older population (68.9 ± 7.9 years) than the typical patient population for TMJDs (20-40 years). It is unclear how ageing affects the structure and biomechanics of the TMJ disc, therefore it is unclear how these results correspond to baseline disc properties of a patient population in an age range typical of TMJDs. Given the small total number of human TMJ discs, and the large natural variation present in human tissues, sex dependencies were unable to be statistically determined with this data set. The large variation present in the results is reflective of the use of tissue samples from an older population with a large age range, and while care was taken to exclude discs considered morphologically abnormal, the sample population also likely included a range of disc conditions. The limited sample size is the result of significant screening efforts selecting healthy temporomandibular articular discs to establish baseline properties within this age group. In addition to donor age, it should be considered that these results correspond to regional properties of the articular disc and not bulk properties. Given the requirements for tensile testing of specimens with near uniform width and thickness, with a suitable long axis for gripping, specimens were dissected from whole TMJ discs. It is possible that specimen preparation diminished overall behavior of the articular disc. Also, it should be noted that during normal loading, while the specimen is stretched over the condylar head, hoop stresses would build up in the anterior and posterior bands of the articular disc, which would have an overall stiffening effect. Biomechanical tests were performed at a single strain rate, therefore, strain rate effects were not considered. However, it has been reported that strain rate effects for collagen tissues, including the TMJ disc, are negligible (Beatty et al., 2001; Fung, 1993). It is expected that the strain rate used in this study is similar to physiologic strain rates, and has been used previously (Beatty et al., 2001; Detamore and Athanasiou, 2003; Matuska et al., 2016). The range of strain implemented in this study may be beyond physiologic limits suggested for the TMJ disc, less than 20% (Beek et al., 2001; Koolstra and van Eijden, 2005, 2007). This is supported by Young's Modulus plateauing between 15-20% strain, before decreasing either due to specimen failures mid-body or specimen slippage. It is anticipated that these results bracket the physiologic response preceding mechanical injury to the TMJ disc.

In conclusion, human TMJ discs demonstrated strong direction and region dependent variations in biomechanical response. Additionally, female articular discs all trended to be stiffer and relax less than male discs, suggesting a possible etiological factor in the

development and progression of TMJDs, and the increased prevalence of TMJDs among women. Physiologically significant differences in tissue mechanical quality, predictive of TMJD development and progression, are unknown. Using second-harmonic generation microscopy, this study also demonstrated human TMJ disc biomechanical response is highly dependent upon regional differences in collagen fiber orientation and organization, with increased stiffness in directions corresponding to high fiber alignment, similar to porcine discs. These findings are important for establishing human TMJ disc biomechanical response and structure-function relationships between collagen fiber direction and organization, and may provide some insights into the clinical prevalence of TMJDs among women.

ACKNOWLEDGEMENTS

REFERENCES

Ahmad M, Hollender L, Anderson Q, Kartha K, Ohrbach R, Truelove EL, John MT, Schiffman EL. Research diagnostic criteria for temporomandibular disorders (RDC/TMD): development of image analysis criteria and examiner reliability for image analysis. Oral surgery, oral medicine, oral pathology, oral radiology, and endodontics. 2009; 107:844–860.

Beatty MW, Bruno MJ, Iwasaki LR, Nickel JC. Strain rate dependent orthotropic properties of pristine and impulsively loaded porcine temporomandibular joint disk. J Biomed Mater Res. 2001; 57:25–34. [PubMed: 11416845]

Beek M, Aarnts MP, Koolstra JH, Feilzer AJ, van Eijden TM. Dynamic properties of the human temporomandibular joint disc. J Dent Res. 2001; 80:876–880. [PubMed: 11379888]

Chen X, Nadiarynkh O, Plotnikov S, Campagnola PJ. Second harmonic generation microscopy for quantitative analysis of collagen fibrillar structure. Nat Protoc. 2012; 7:654–669. [PubMed: 22402635]

Choukas NC, Sicher H. The structure of the temporomandibular joint. Oral Surg Oral Med Oral Pathol. 1960; 13:1203–1213. [PubMed: 13693302]

Detamore MS, Athanasiou KA. Tensile Properties of the Porcine Temporomandibular Joint Disc. Journal of Biomechanical Engineering. 2003; 125:558. [PubMed: 12968581]

Elliott DM, Setton LA. Anisotropic and inhomogeneous tensile behavior of the human anulus fibrosus: experimental measurement and material model predictions. J Biomech Eng. 2001; 123:256–263. [PubMed: 11476369]

Ford KR, Myer GD, Hewett TE. Longitudinal effects of maturation on lower extremity joint stiffness in adolescent athletes. The American journal of sports medicine. 2010a; 38:1829–1837. [PubMed: 20522830]

Ford KR, Shapiro R, Myer GD, Van Den Bogert AJ, Hewett TE. Longitudinal sex differences during landing in knee abduction in young athletes. Medicine and science in sports and exercise. 2010b; 42:1923–1931. [PubMed: 20305577]

Fung, YC. Biomechanics: Mechanical Properties of Living Tissues. 2nd. Springer-Verlag; New York: 1993.

Gallo LM, Nickel JC, Iwasaki LR, Palla S. Stress-field translation in the healthy human temporomandibular joint. J Dent Res. 2000; 79:1740–1746. [PubMed: 11077988]

Griffin CJ, Hawthorn R, Harris R. Anatomy and histology of the human temporomandibular joint. Monogr Oral Sci. 1975; 4:1–26. [PubMed: 1097895]

Griffin LY, Agel J, Albohm MJ, Arendt EA, Dick RW, Garrett WE, Garrick JG, Hewett TE, Huston L, Ireland ML, Johnson RJ, Kibler WB, Lephart S, Lewis JL, Lindenfeld TN, Mandelbaum BR, Marchak P, Teitz CC, Wojtys EM. Noncontact anterior cruciate ligament injuries: risk factors and

prevention strategies. The Journal of the American Academy of Orthopaedic Surgeons. 2000; 8:141–150. [PubMed: 10874221]

Hansson T, Oberg T, Carlsson GE, Kopp S. Thickness of the soft tissue layers and the articular disk in the temporomandibular joint. Acta Odontol Scand. 1977; 35:77–83. [PubMed: 266827]

Haskin CL, Milam SB, Cameron IL. Pathogenesis of degenerative joint disease in the human temporomandibular joint. Crit Rev Oral Biol Med. 1995; 6:248–277. [PubMed: 8785264]

Herring SW, Decker JD, Liu ZJ, Ma T. Temporomandibular joint in miniature pigs: anatomy, cell replication, and relation to loading. Anat Rec. 2002; 266:152–166. [PubMed: 11870598]

Holm S. A simple sequentially rejective multiple test procedure. Scandinavian Journal of Statistics. 1979; 6:65–70.

Houle MA, Couture CA, Bancelin S, Van der Kolk J, Auger E, Brown C, Popov K, Ramunno L, Legare F. Analysis of forward and backward Second Harmonic Generation images to probe the nanoscale structure of collagen within bone and cartilage. J Biophotonics. 2015; 8:993–1001. [PubMed: 26349534]

Hughes G, Watkins J, Owen N. Gender differences in lower limb frontal plane kinematics during landing. Sports biomechanics / International Society of Biomechanics in Sports. 2008; 7:333–341.

Jagger RG. The surface structure of the temporomandibular joint disk: a scanning electron microscopic study. J Oral Rehabil. 1980; 7:225–234. [PubMed: 6931198]

Kalpakci KN, Willard VP, Wong ME, Athanasiou KA. An interspecies comparison of the temporomandibular joint disc. J Dent Res. 2011; 90:193–198. [PubMed: 21118792]

Kernozek TW, Torry MR, Cowley H, Tanner S. Gender differences in frontal and sagittal plane biomechanics during drop landings. Medicine and science in sports and exercise. 2005; 37:1003–1012. H, V.A.N.H. discussion 1013. [PubMed: 15947726]

Koolstra JH, van Eijden TM. Combined finite-element and rigid-body analysis of human jaw joint dynamics. J Biomech. 2005; 38:2431–2439. [PubMed: 16214491]

Koolstra JH, van Eijden TM. Consequences of viscoelastic behavior in the human temporomandibular joint disc. J Dent Res. 2007; 86:1198–1202. [PubMed: 18037655]

Lawrence, JS. The epidemiology of degenerative joint disease: Occupational and ergonomic aspects. In: Helminen, HJ., editor. Joint Loading: Biology and Health of Articular Fractures. Butterworth-Heinemann Ltd; Oxford, UK: 1987. p. 316-351.

LeResche L. Epidemiology of temporomandibular disorders: implications for the investigation of etiologic factors. Crit Rev Oral Biol Med. 1997; 8:291–305. [PubMed: 9260045]

Lilledahl M, Olderøy M, Finnøy A, Olstad K, Brinchman JE. Second harmonic generation imaging in tissue engineering and cartilage pathologies. Proc of SPIE 9329, Multiphoton Microscopy in the Biomedical Sciences XV. 2015

Matuska AM, Muller S, Dolwick MF, McFetridge PS. Biomechanical and biochemical outcomes of porcine temporomandibular joint disc deformation. Arch Oral Biol. 2016; 64:72–79. [PubMed: 26774186]

Mills DK, Daniel JC, Herzog S, Scapino RP. An animal model for studying mechanisms in human temporomandibular joint disc derangement. J Oral Maxillofac Surg. 1994; 52:1279–1292. [PubMed: 7965332]

Moskowitz, RW. Osteoarthritis. In: Katz, WA., editor. Diagnosis and management of rheumatic diseases. 2nd. J. B. Lippincott Co; Philadelphia: 1988.

Osborn JW. The disc of the human temporomandibular joint: design, function and failure. J Oral Rehabil. 1985; 12:279–293. [PubMed: 3862791]

Peyron, JG.; Altman, RD. The epidemiology of osteoarthritis. In: Moskowitz, RW.; Howell, DS.; Goldberg, VM.; Mankin, HJ., editors. Osteoarthritis: Diagnosis and Medical/Surgical Management. 2nd. W.B. Saunders; Philadelphia, PA: 1992.

Piette E. Anatomy of the human temporomandibular joint. An updated comprehensive review. Acta stomatologica Belgica. 1993; 90:103–127. [PubMed: 8237635]

Rayne J. Functional anatomy of the temporomandibular joint. Br J Oral Maxillofac Surg. 1987; 25:92–99. [PubMed: 3472599]

Rees LA. The structure and function of the mandibular joint. Br Dent J. 1954; 96:125–133.

Scapino RP. Histopathology associated with malposition of the human temporomandibular joint disc. Oral Surg Oral Med Oral Pathol. 1983; 55:382–397. [PubMed: 6574416]

Schiffman EL, Truelove EL, Ohrbach R, Anderson GC, John MT, List T, Look JO. The Research Diagnostic Criteria for Temporomandibular Disorders. I: overview and methodology for assessment of validity. Journal of orofacial pain. 2010; 24:7–24. [PubMed: 20213028]

Shapiro HH. The anatomy of the temporomandibular joint. Structural relations and therapy. Oral Surg Oral Med Oral Pathol. 1950; 3:1521–1539. [PubMed: 14797281]

Shengyi T, Xu Y. Biomechanical properties and collagen fiber orientation of TMJ discs in dogs: Part 1. Gross anatomy and collagen fiber orientation of the discs. J Craniomandib Disord. 1991; 5:28–34. [PubMed: 1809767]

Shi C, Wright GJ, Ex-Lubeskie CL, Bradshaw AD, Yao H. Relationship between anisotropic diffusion properties and tissue morphology in porcine TMJ disc. Osteoarthritis Cartilage. 2013; 21:625–633. [PubMed: 23353670]

Taguchi N, Nakata S, Oka T. Three-dimensional observation of the temporomandibular joint disk in the rhesus monkey. J Oral Surg. 1980; 38:11–15. [PubMed: 6765973]

Tanaka E, Shibaguchi T, Tanaka M, Tanne K. Viscoelastic properties of the human temporomandibular joint disc in patients with internal derangement. J Oral Maxillofac Surg. 2000; 58:997–1002. [PubMed: 10981980]

Tanaka E, Tanaka M, Hattori Y, Aoyama J, Watanabe M, Sasaki A, Sugiyama M, Tanne K. Biomechanical behaviour of bovine temporomandibular articular discs with age. Arch Oral Biol. 2001; 46:997–1003. [PubMed: 11543706]

Tanaka E, van Eijden T. Biomechanical behavior of the temporomandibular joint disc. Crit Rev Oral Biol Med. 2003; 14:138–150. [PubMed: 12764076]

Tanne K, Tanaka E, Sakuda M. The elastic modulus of the temporomandibular joint disc from adult dogs. J Dent Res. 1991; 70:1545–1548. [PubMed: 1774386]

Wang M, Cao H, Ge Y, Widmalm SE. Magnetic resonance imaging on TMJ disc thickness in TMD patients: a pilot study. The Journal of prosthetic dentistry. 2009; 102:89–93. [PubMed: 19643222]

Warren MP, Fried JL. Temporomandibular disorders and hormones in women. Cells Tissues Organs. 2001; 169:187–192. [PubMed: 11455113]

Wright GJ, Kuo J, Shi C, Bacro TR, Slate EH, Yao H. Effect of mechanical strain on solute diffusion in human TMJ discs: an electrical conductivity study. Ann Biomed Eng. 2013; 41:2349–2357. [PubMed: 23771300]
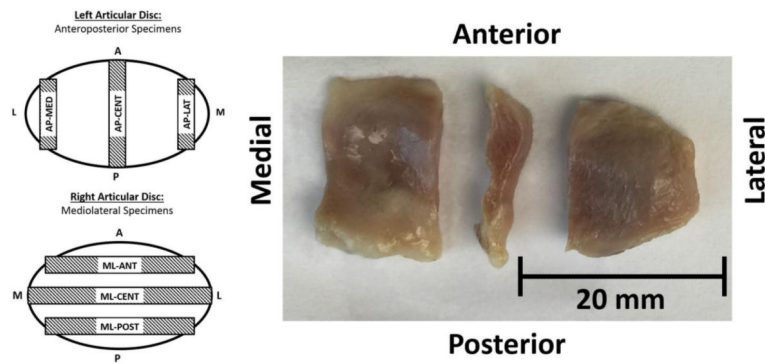
Figure 1.
Tensile test specimens were taken at three positions from each articular disc. Left articular discs were used for all specimens in the anteroposterior direction, with specimens taken at medial (AP-MED), central (AP-CENT), and lateral (AP-LAT) regions. Right articular discs were used for all specimens in the mediolateral direction, with specimens taken at anterior (ML-ANT), central (ML-CENT), and posterior (ML-POST) regions. Specimens were prepared by dissecting 2 mm strips equally spaced from temporomandibular joints, and specimen biconcavity was removed prior to testing.
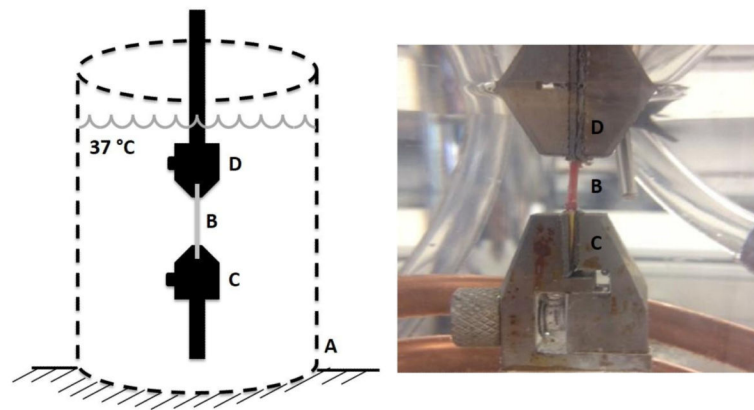
Figure 2.
Tensile stress relaxation tests were performed using a materials tests system, with specimens in a custom enclosed temperature controlled saline bath (A) maintained at a constant 37 °C. Test specimens (B) were held by tensile clamps (C and D) with fine-grit sandpaper.
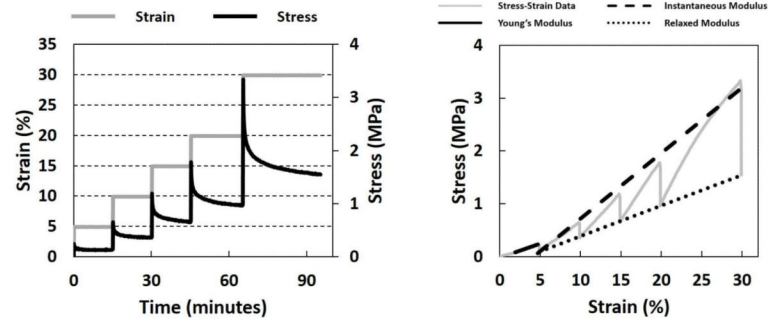
Figure 3.
Left: Incremental step-strains (gray line) were applied to specimens with strain increments of 5%, 10%, 15%, 20% and 30%, with relaxation periods of 15, 15, 15, 20, and 30 minutes, respectively. Right: Young's Modulus, Instantaneous Modulus and Relaxed Modulus were calculated from constructed stress-strain curves (solid gray line) for each stress-relaxation experiment. Young's Modulus (solid black line) was calculated as the slope of the best fit line through 40-100% of the stress-strain response during the ramp loading phase, for each strain increment. Instantaneous Modulus (black dashed line) and Relaxed Modulus (black dotted line) were calculated as the slope of the best fit lines through the local peaks of the stress-strain curves and the end of each stress-relaxation phase, respectively.
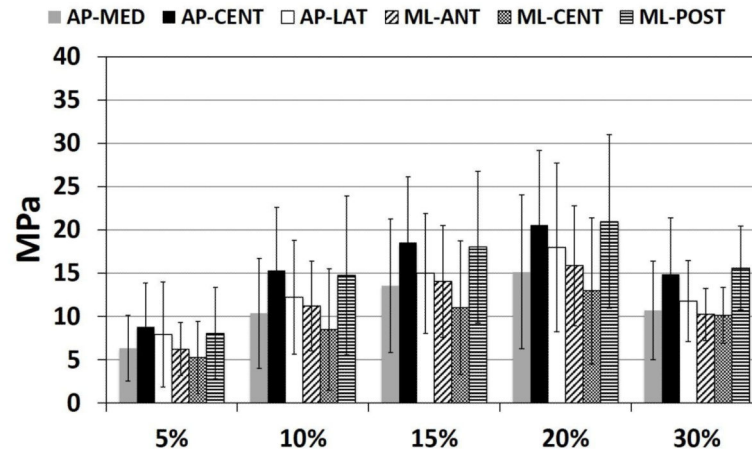
Figure 4.
Young's Modulus at each strain increment (5%, 10%, 15%, 20% and 30%), for each region in the AP direction (AP-MED, AP-CENT, AP-LAT) and ML direction (ML-ANT, ML-CENT, ML-POST). Young's Modulus increased with increasing strain increment from 5% to 20% strain, before decreasing at 30% strain. All pairwise comparisons between strain increments were significant, except for between 15-20% and 10-30% strain which were not statistically different: 5% vs 10%, $p<0.001$; 5% vs 15%, $p<0.001$; 5% vs 20%, $p<0.001$; 5% vs 30%, $p<0.001$; 10% vs 15%, $p<0.001$; 10% vs 20%, $p<0.001$; 10% vs 30%, $p=0.985$; 15% vs 20%, $p=0.087$; 15% vs 30%, $p=0.039$; 20% vs 30%, $p<0.001$.
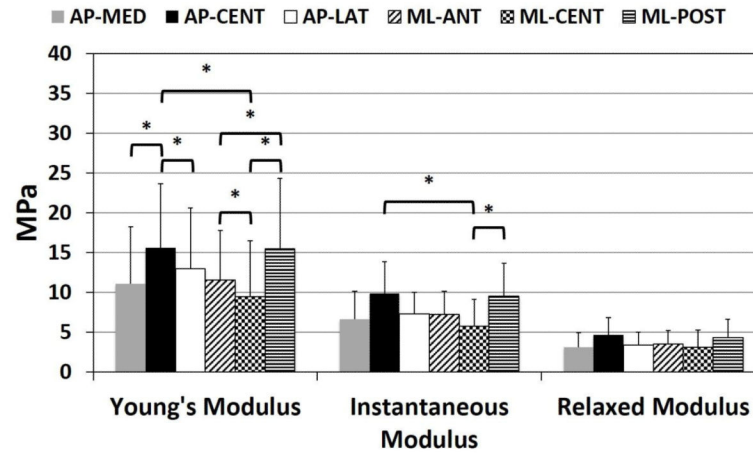
Figure 5.
Young's Modulus adjusted for strain increment, Instantaneous Modulus and Relaxed Modulus for each region in the AP direction (AP-MED, AP-CENT, AP-LAT) and ML direction (ML-ANT, ML-CENT, ML-POST). Young's Modulus showed significant differences by region (p<0.001). In the anteroposterior direction, Young's Modulus was significantly higher in the AP-CENT region compared to both AP-LAT (p=0.04) and AP-MED (p<0.001) regions. In the mediolateral direction, Young's Modulus, adjusted for strain increment, was significantly lower in the ML-CENT region compared to both ML-POST (p<0.001) and ML-ANT (p=0.04) regions, and ML-ANT was significantly less than ML-POST (p=0.04). In the central region of the articular disc, Young's Modulus was significantly higher in the anteroposterior direction compared to the mediolateral direction (p=0.04). Differences in Instantaneous Modulus by region were significant (p=0.007). Anteroposteriorly, AP-CENT specimens had a higher Instantaneous Modulus compared to AP-MED specimens, however not significantly (p=0.068). In the mediolateral direction, ML-POST specimens had a significantly higher Instantaneous Modulus compared to ML-CENT specimens (p=0.002). In the central region of the articular disc, Instantaneous Modulus was significantly higher in the anteroposterior direction compared to the mediolateral direction (p=0.001). Differences in Relaxed Modulus by region were not significant (p=0.094).
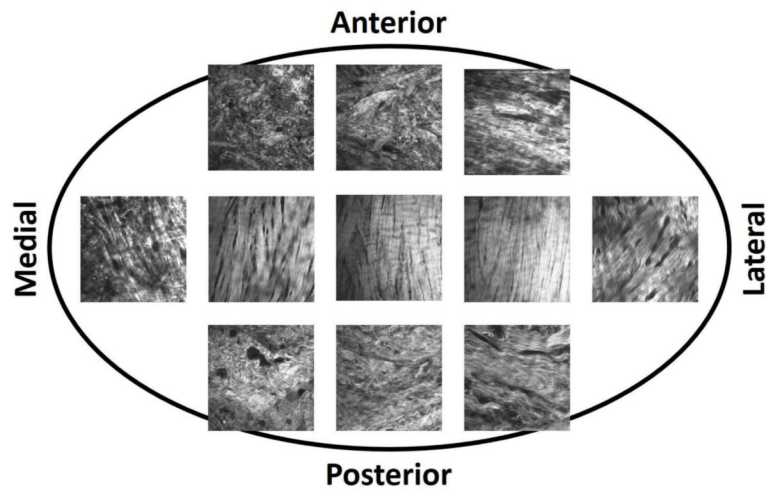
Figure 6.
Second-harmonic generation microscopy images of the superior surface of an unstained, intact human TMJ disc taken from a 73 year old female cadaveric donor. Throughout the articular disc, collagen fibers are predominately oriented anteroposteriorly. In the central region of the disc, fibers are tightly organized. Towards the medial aspect of the disc, fibers remain predominately anterorposteriorly oriented, but fiber overall fiber organization decreases with fibers becoming loosely interwoven. On the lateral aspect of the disc, anterorposterior fibers are interwoven with mediolaterally directed fibers, in a more tight-knit organization. In the anterior and posterior bands, fibers run predominately mediolaterally, with anteroposterior fibers interwoven in a dense arrangement.

Author Manuscript

Table 1

...nsile biomechanical response categorized by direction and region for Young's Modulus, Instantaneous Modulus and Relaxed Modulus for ...romandibular joint discs, mean (std.dev).

	Average Young's Modulus (MPa)						Instantaneous Modulus (MPa)						Relaxed Modulus (MPa)					
	AP-CENT	...MED	AP-LAT	ML-ANT	ML-CENT	ML-POST	AP-MED	AP-CENT	AP-LAT	ML-ANT	ML-CENT	ML-POST	AP-MED	AP-CENT	AP-LAT	ML-ANT	ML-CENT	ML-POST
	18.9 (8.5)		13.6 (6.2)	12.9 (7.5)	12.1 (8.6)	15.3 (9.9)	8.3 (4.2)	8.5 (2.9)	7.2 (4.0)	9.0 (5.2)	5.4 (2.9)	10.8 (6.5)	3.1 (0.8)	1.9 (1.7)	2.7 (1.7)	3.4 (2.0)	1.4 (1.3)	4.3 (3.0)
	13.1 (6.8)		12.3 (?.9)	10.4 (4.6)	7.3 (4.3)	15.6 (7.7)	4.0 (0.8)	7.3 (5.0)	4.7 (1.9)	16.3 (13.7)	3.2 (1.2)	7.8 (4.6)	1.8 (0.5)	2.0 (2.0)	1.7 (0.8)	6.2 (4.8)	1.4 (0.6)	3.1 (2.0)

Table 2

Tensile biomechanical properties (Young's Modulus, Instantaneous Modulus and Relaxed Modulus) for temporomandibular joint discs reported in the literature and from the present study.

Study Reference	Species	Strain Rate(s)	Strain Magnitude(s)	Young's Modulus	Instantaneous Modulus	Relaxed Modulus
Shengyi et al., 1991	Canine (N=8)	Impulse load	Strain up to 10%	--	ML-ANT: 200 MPa MP-CENT: 47 MPa ML-POST: 234 MPa	ML-ANT: 30 MPa ML-CENT: 18 MPa ML-POST: 30 MPa
Tanne et al., 1991	Canine (N=6)	0.1 N/s	Strain up to 3.5 MPa	AP-MED: 92 MPa AP-CENT: 101 MPA AP-LAT: 84 MPa	--	--
Tanaka et al., 2000	Human (N=7)	0.02 mm/sec	Increments up to 4 MPa	--	Healthy-ML: 96 MPa TMJD-ML: 96 MPa	Healthy, ML: 61 MPa Internal Der., ML: 59 MPa
Beatty et al., 2001	Porcine (N=10)	0.0083 mm/sec 0.83 mm/sec 8.3 mm/sec	Strain to failure	AP@0.0083 mm/sec: 27 MPa AP@8.3 mm/sec: 76 MPa ML@8.3 mm/sec: 3 MPa	--	--
Tanaka et al., 2001	Bovine (N=40)	1.04 mm/sec	Strain up to 1.0 MPa and 1.5 MPa	AP-MED: 26 MPa AP-CENT: 23 MPa AP-LAT: 24 MPa	--	--
Detamore et al., 2003	Porcine (N=6)	6 mm/min	Strain to failure in increments of 5%, 10%, 15%, 20%, 25%, 35% …	--	AP-MED: 24 MPa AP-CENT: 29 MPa AP-LAT: 18 MPa ML-ANT: 15 MPa ML-CENT: 1 MPa ML-POST: 32 MPa	AP-MED: 14 MPa AP-CENT: 19 MPa AP-LAT: 11 MPa ML-ANT: 9 MPa ML-CENT: 0.6 MPa ML-POST: 23 MPa
Wang et al., 2014	Rat (N=6)	Not specified	30% strain	--	AP: 3 MPa ML: 2: MPa	AP: 1 MPa ML: 0.2 MPa
Matuska et al., 2016	Porcine (N=12)	1% strain/sec	Strain to failure	AP-MED: 65 MPa AP-CENT: 140 MPa AP-LAT: 45 MPa	--	--
Present Study	Human (N=12)	1% strain/sec	5%, 10%, 15%, 20% and 30%	AP-MED: 11 MPa AP-CENT:16 MPa AP-LAT: 13 MPa ML-ANT: 12 MPa ML-CENT: 9 MPa ML-POST: 15 MPa	AP-MED: 7 MPa AP-CENT: 10 MPa AP-LAT: 7 MPa ML-ANT: 7 MPa ML-CENT: 6 MPa ML-POST: 10 MPa	AP-MED: 3 MPa AP-CENT: 5 MPa AP-LAT: 3 MPa ML-ANT: 4 MPa ML-CENT: 3 MPa ML-POST: 4
Present Study	Human (N=12)	1% strain/sec	5%, 10%, 15%, 20% and 30%	AP-MED: 11 MPa AP-CENT:16 MPa AP-LAT: 13 MPa ML-ANT: 12 MPa ML-CENT: 9 MPa ML-POST: 15 MPa	AP-MED: 7 MPa AP-CENT: 10 MPa AP-LAT: 7 MPa ML-ANT: 7 MPa ML-CENT: 6 MPa ML-POST: 10 MPa	AP-MED: 3 MPa AP-CENT: 5 MPa AP-LAT: 3 MPa ML-ANT: 4 MPa ML-CENT: 3 MPa ML-POST: 4